

Energy Storage System Based Dynamic Voltage Restorer Framework to Improve Power Quality of the Distribution Grid

V. Yuvaaj & D . Sreenivasula reddy

PG Student, Department of EEE, SVEC, Tirupati
M.Tech, Assit.Prof, Department of EEE, SVCE, Tirupati

Abstract: *Quality of the output power delivered from the utilities has become a major concern of the modern industries for the last decade. These power quality associated problems are voltage sag, surge, flicker, voltage imbalance, interruptions and harmonic problems. To overcome the problems caused by customer side abnormalities so called custom power devices are connected closer to the load end. One such reliable customer power device used to address the voltage sag, swell problem is the Dynamic Voltage Restorer (DVR). It is a series connected custom power device, which is considered to be a cost effective alternative when compared with other commercially available voltage sag compensation devices. With the integration of ultra-capacitors (UCAP) with the DVR&Fuzzy Logic Controller (FLC), the UCAP-DVR system will have active power capability and will be able to independently compensate temporary voltage sags and swells without relying on the grid. The proposed system helps in providing a stiff dc-link voltage, and the integrated UCAP-DVR-FLC system helps in compensating temporary voltage sags and voltage swells. The MATLAB/SIMULINK power system tool box has been used to develop the proposed system.*

Index Terms—DC-DC converter, $d-q$ control, DSP, dynamic voltage restorer (DVR), FLC Controller, energy storage integration, phase locked loop (PLL), sag/swell, Ultracapacitor (UCAP).

1 Introduction

The electric power system is considered to be composed of three functional blocks - generation, transmission and distribution. For a reliable power system, the generation unit must produce adequate power to meet customer's demand, transmission systems must transport bulk power over long distances without overloading or jeopardizing system stability and distribution systems must deliver electric power to each

customer's premises from bulk power systems. Distribution system locates the end of power system and is connected to the customer directly, so the power quality mainly depends on distribution system. The reason behind this is that the electrical distribution network failures account for about 90% of the average customer interruptions. In the earlier days, the major focus for power system reliability was on generation and transmission only as these more capital cost is involved in these. In addition their insufficiency can cause widespread catastrophic consequences for both society and its environment. But now a day's distribution systems have begun to receive more attention for reliability assessment.

Initially for the improvement of power quality or reliability of the system FACTS devices like static synchronous compensator (STATCOM), static synchronous series compensator (SSSC), interline power flow controller (IPFC), and unified power flow controller (UPFC) etc are introduced. These FACTS devices are designed for the transmission system. But now a day's more attention is on the distribution system for the improvement of power quality, these devices are modified and known as custom power devices. The main custom power devices which are used in distribution system for power quality improvement are distribution static synchronous compensator (DSTATCOM), dynamic voltage Restorer (DVR), active filter (AF), unified power quality conditioner (UPQC) etc.

In this thesis work from the above custom power devices, DVR is used with PI controller for the power quality improvement in the distribution system. Here two different loads are considered, one is linear load and the other is induction motor. Different fault conditions are considered with these loads to analyze the operation of DVR to improve the power quality in distribution system.

2 Three Phase Series Inverter

2.1. Power Stage

The one-line diagram of the system is shown in Fig. 1. The power stage is a three-phase voltage source inverter, which is connected in series to the grid and is responsible for compensating the voltage sags and swells; the model of the series DVR and its controller is shown in Fig. 2. The inverter system consists of an insulated gate bipolar transistor (IGBT) module, its gate-driver, LC filter, and an isolation transformer. The dc-link voltage V_{dc} is regulated at 260 V for optimum performance of the converter and the line–line voltage V_{abis} 208 V; based on these, the modulation index m of the inverter is given by

$$m = \frac{2\sqrt{2}}{\sqrt{3}V_{dc} * n} V_{ab(rms)} \quad (1)$$

When n is the turns ratio of the isolation transformer. Substituting n as 2.5 in (1), the required modulation index is calculated as 0.52. Therefore, the output of the dc–dc converter should be regulated at 260 V for providing accurate voltage compensation. The objective of the integrated UCAPDVR system with active power capability is to compensate for *temporary voltage sag* (0.1–0.9 p.u.) and *voltage swell* (1.1–1.2 p.u.), which last from 3 s to 1 min [15].

2.2. Controller Implementation

There are various methods to control the series inverter to provide dynamic voltage restoration and most of them rely on injecting a voltage in quadrature with advanced phase, so that reactive power is utilized in voltage restoration [3]. Phase advanced voltage restoration techniques are complex in implementation, but the primary reason for using these techniques is to minimize the active power support and thereby the amount of energy storage requirement at the dc-link in order to minimize the cost of energy storage. However, the cost of energy storage has been declining and with the availability of *active power support* at the dc-link, complicated phase-advanced techniques can be avoided and voltages can be injected *in-phase* with the system voltage during voltage sag or a swell

event. The control method requires the use of a PLL to find the rotating angle. As discussed previously, the goal of this project is to use the *activepower capability* of the UCAP-DVR system and compensate temporary voltage sags and swells.

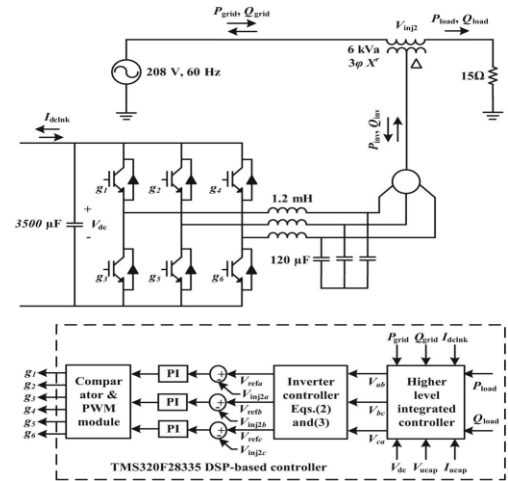


Fig. 2. Model of three-phase series inverter (DVR) and its controller with integrated higher order controller.

The inverter controller implementation is based on injecting voltages *in-phase* with the supply-side line–neutral voltages. This requires PLL for estimating θ , which has been implemented using the *fictitious power method* described in [18].

Based on the estimated θ and the line–line source voltages, V_{ab} , V_{bc} , and V_{ca} (which are available for this delta-sourced system) are transformed into the d – q domain and the line–neutral components of the source voltage V_{sa} , V_{sb} , and V_{sc} , which are not available, can then be estimated using

$$\begin{bmatrix} V_{sa} \\ V_{sb} \\ V_{sc} \end{bmatrix} = \begin{bmatrix} 1 & 0 \\ -\frac{1}{2} & \frac{\sqrt{3}}{2} \\ -\frac{1}{2} & -\frac{\sqrt{3}}{2} \end{bmatrix} \begin{bmatrix} \cos(\theta - \frac{\pi}{6}) & \sin(\theta - \frac{\pi}{6}) \\ -\sin(\theta - \frac{\pi}{6}) & \cos(\theta - \frac{\pi}{6}) \end{bmatrix} \begin{bmatrix} \frac{V_d}{\sqrt{3}} \\ \frac{V_q}{\sqrt{3}} \end{bmatrix} \quad (2)$$

$$\begin{bmatrix} V_{refa} \\ V_{refb} \\ V_{refc} \end{bmatrix} = m * \begin{bmatrix} (\sin \theta - \frac{V_{sa}}{169.7}) \\ (\sin(\theta - \frac{2\pi}{3}) - \frac{V_{sb}}{169.7}) \\ (\sin(\theta + \frac{2\pi}{3}) - \frac{V_{sc}}{169.7}) \end{bmatrix} \quad (3)$$

$$P_{inv} = 3V_{inj2a(rms)} I_{La(rms)} \cos \varphi$$

$$Q_{inv} = 3V_{inj2a(rms)} I_{La(rms)} \sin \varphi. \quad (4)$$

3UCAP& Bidirectional DC – Dc Converter with FLC

3.1. UCAP Setup

The choice of the number of UCAPs necessary for providing grid support depends on the amount of support needed, terminal voltage of the UCAP, dc-link voltage, and distribution grid voltages. In this paper, the experimental setup consists of three 48 V, 165F UCAPs (BMOD0165P048) manufactured by Maxwell Technologies, which are connected in series. Therefore, the terminal voltage of the UCAP bank is 144 V and the dc-link voltage is programmed to 260 V. This would give the dc–dc converter a practical operating duty ratio of 0.44–0.72 in the *boost mode* while the UCAP is discharging and 0.27–0.55 in the *buck mode* while the UCAP is charging from the grid through the dc-link and the dc–dc converter. It is practical and cost-effective to use three modules in the UCAP bank.

Assuming that the UCAP bank can be discharged to 50% of its initial voltage ($V_{uc,ini}$) to final voltage ($V_{uc,fin}$) from 144 to 72 V, which translates to depth of discharge of 75%, the energy in the UCAP bank available for discharge is given by

$$E_{UCAP} = \frac{1}{2} * C * \frac{(V_{uc,ini}^2 - V_{uc,fin}^2)}{60} W - \text{min} \quad (5)$$

$$E_{UCAP} = 1/2 * 165 / 3 * (144^2 - 72^2) / 60$$

$$= 7128 W - \text{min.}$$

3.2. Bidirectional DC–DC Converter and Controller

A UCAP cannot be directly connected to the dc-link of the inverter like a battery, as the voltage profile of the UCAP varies as it discharges energy. Therefore, there is a need to integrate the UCAP system through a bidirectional dc–dc converter, which maintains a stiff dc-link voltage, as the UCAP voltage decreases while *discharging* and increases while *charging*. The model of the bidirectional dc–dc converter and its controller are shown in Fig. 3, where the input consists of three UCAPs connected in series and the output consists of a nominal load of 213.5 Ω to prevent operation at no-load, and the output is connected to the dc-link of the inverter. The

amount of active power support required by the grid during a voltage sag event is dependent on the depth and duration of the voltage sag, and the dc–dc converter should be able to withstand this power during the *discharge* mode. The dc–dc converter should also be able to operate in bidirectional mode to be able to *charge* or absorb additional power from the grid during voltage swell event. In this paper, the bidirectional dc–dc converter acts as a boost converter while *discharging* power from the UCAP and acts as a buck converter while *charging* the UCAP from the grid.

A bidirectional dc–dc converter is required as an interface between the UCAP and the dc-link since the UCAP voltage varies with the amount of energy discharged while the dc-link voltage has to be stiff. Therefore, the bidirectional dc–dc converter is designed to operate in boost mode when the UCAP bank voltage is between 72 and 144 V and the output voltage is regulated at 260 V. When the UCAP bank voltage is below 72 V, the bidirectional dc–dc converter is operated in buck mode and draws energy from the grid to charge the UCAPs and the output voltage is again regulated at 260 V.

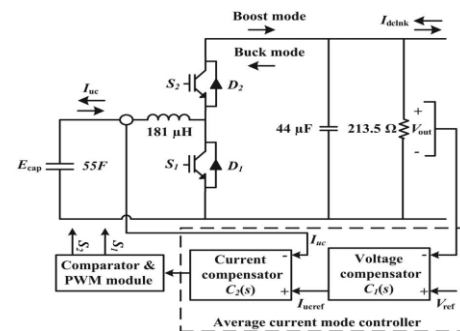


Fig. 3. Model of the bidirectional dc–dc converter and its controller.

Average current mode control, which is widely explored in literature [19], is used to regulate the output voltage of the bidirectional dc–dc converter in both *buck* and *boost* modes while *charging* and *discharging* the UCAP bank. This method tends to be more stable when compared to other methods such as voltage mode control and peak current mode control. Average current mode controller is shown in Fig. 3, where the dc-link and actual output voltage V_{out} is compared with the reference voltage

V_{ref} and the error is passed through the voltage compensator $C1(s)$, which generates the average reference current I_{uref} . When the inverter is *discharging* power into the grid during voltage sag event, the dc-link voltage V_{out} tends to go below the reference V_{ref} and the error is positive; I_{uref} is positive and the dc–dc converter operates in *boost* mode. When the inverter is absorbing power from the grid during voltage swell event or *charging* the UCAP, V_{out} tends to increase above the reference V_{ref} and the error is negative; I_{uref} is negative and the dc–dc converter operates in *buck* mode. Therefore, the sign of the error between V_{out} and V_{ref} determines the sign of I_{uref} and thereby the direction of operation of the bidirectional dc–dc converter. The reference current I_{uref} is then compared to the actual UCAP current (which is also the inductor current) I_{uc} and the error is then passed through the current compensator $C2(s)$. The compensator transfer functions, which provide a stable response, are given by

$$C_1(s) = 1.67 + \frac{23.81}{s} \quad (6)$$

$$C_2(s) = 3.15 + \frac{1000}{s} \quad (7)$$

4. Fuzzy Logic Controller

Fuzzy logic uses fuzzy set theory, in which a variable is member of one or more sets, with a specified degree of membership. Fuzzy logic allow us to emulate the human reasoning process in computers, quantify imprecise information, make decision based on vague and in complete data, yet by applying a “defuzzification” process, arrive at definite conclusions.

The FLC mainly consists of three blocks

- Fuzzification
- Inference
- Defuzzification

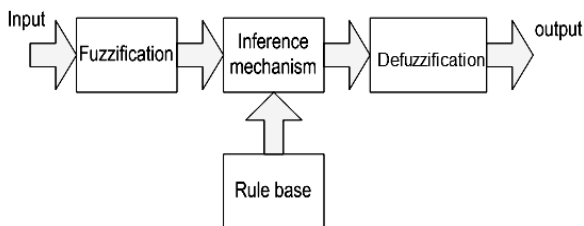


Fig. 4 Block Diagram of a Fuzzy Logic Controller

RULES:

If input is NEGATIVE then output is POSITIVE

If input is ZERO then output is ZERO
If input is POSITIVE then output is NEGATIVE

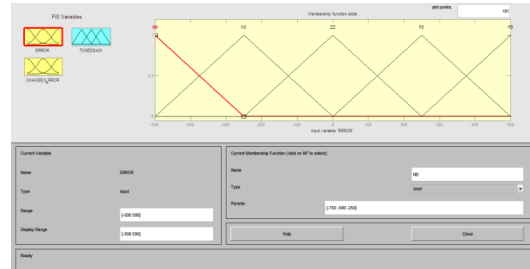


Fig..5 Fuzzy Inputs and Outputs

5. Simulation circuits and results for proposed system:

In proposed system we are using two controllers:

1. Fuzzy logic controller is used in DC-DC converter and
2. PI controller is used in DVR

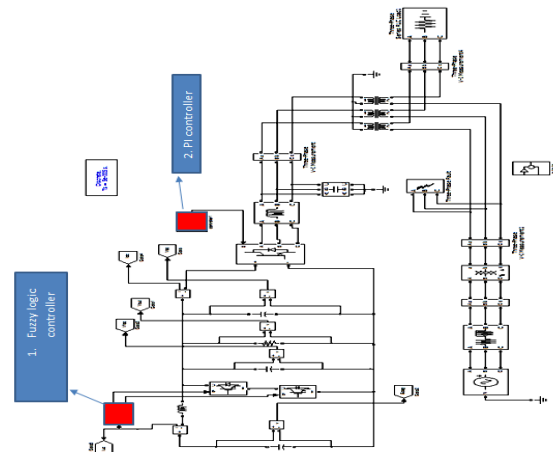


Fig.6Matlab/Simulink model for proposed system

5.1 Controller implementation of DVR:

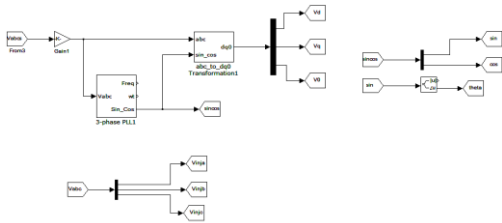


Fig.7 Controller implementation of DVR

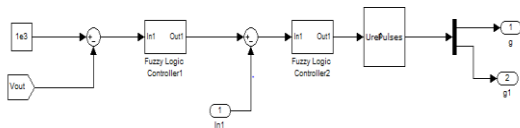


Fig.8 Controller implementation of DC-DC converter

5.2 Waveforms during voltage sag:

5.2.1 Peak voltages during sag:

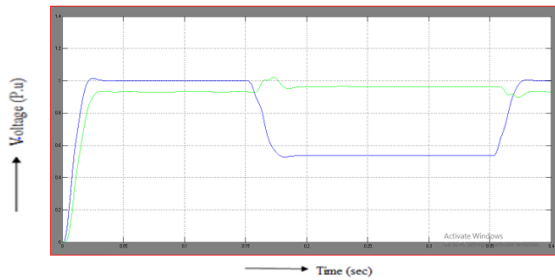


Fig.9 Source and load peak voltages V_{Smax} (Blue) and V_{Lmax} during sag(Green).

5.2.2 Sag voltage:

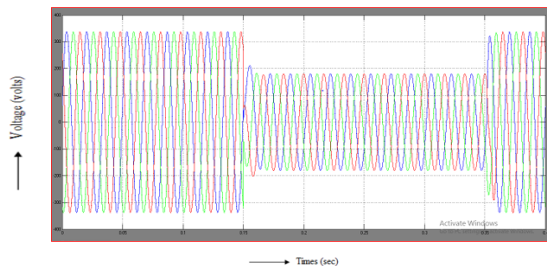


Fig.10 Source voltages V_{sa} (blue), V_{sb} (red), and V_{sc} (green) during sag

5.2.3 DVR injected voltage:

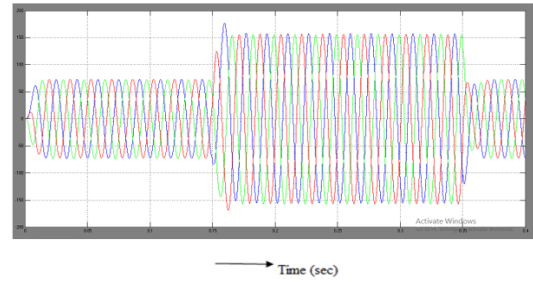


Fig.11 Injected voltages V_{inj2a} (blue), V_{inj2b} (red), and V_{inj2c} (green) during sag

5.2.4 Load voltage:

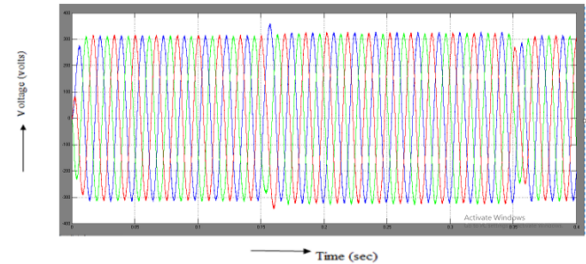


Fig.12 Load voltages V_{La} (blue), V_{Lb} (red), and V_{Lc} (green) during sag

5.9.5 Voltages of capacitors:

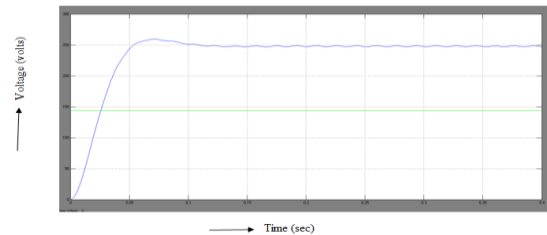


Fig.13 Voltages of dc-dc converter in Capacitor $44\mu F$ (Blue) and Capacitor $55F$ (Green) during voltage sag

5.2.6 Currents of capacitors:

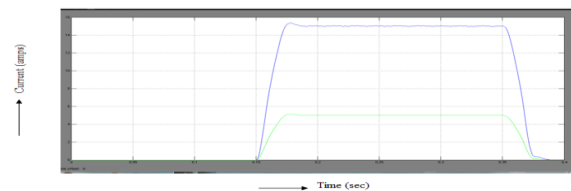


Fig.14 Ultra-capacitor current I_{uc} (Blue) and Capacitor current I_{dc} of DC-DC Converter (Green) of dc-dc converter during voltage sag

5.2.7 Comparison of DVR voltage and system voltage:

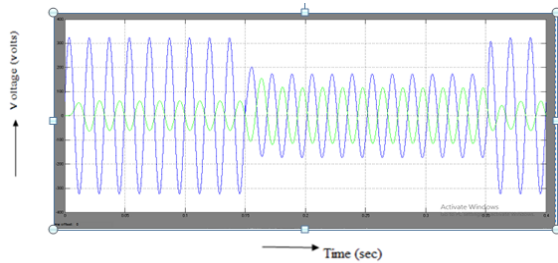


Fig.15 V_{inj2a} (green) and V_{sa} (blue) waveforms during sag

5.2.8 Active powers and RMS product of capacitor current and voltage UCAP:

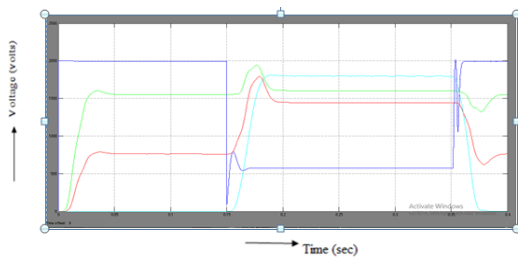


Fig.16 Active power of grid (Blue), Load (Green), inverter (Red) and RMS product of Capacitor current I_{dc} (DC-DC converter) and Ultra-capacitor voltage V_{dc} (Light blue) during voltage sag

5.3 Waveforms during voltage swell:

5.3.1 Peak voltages during swell:

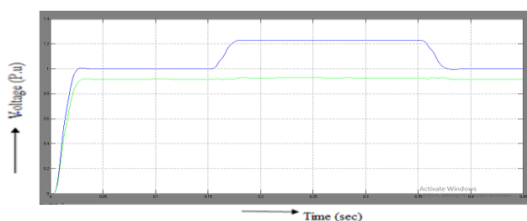


Fig.17 Source and load peak voltages V_{Smax} (Blue) and V_{Lmax} (Green) during swell

5.3.2 Swell voltage:

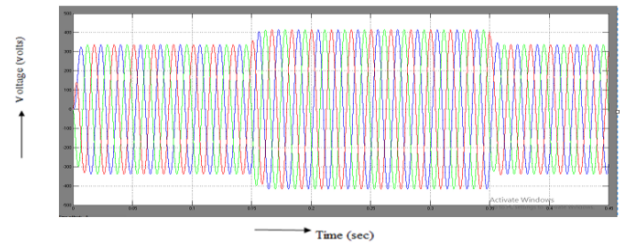


Fig.18 Source voltages V_{sa} (blue), V_{sb} (red), and V_{sc} (green) during swell

5.3.3 DVR absorbed voltage during swell:

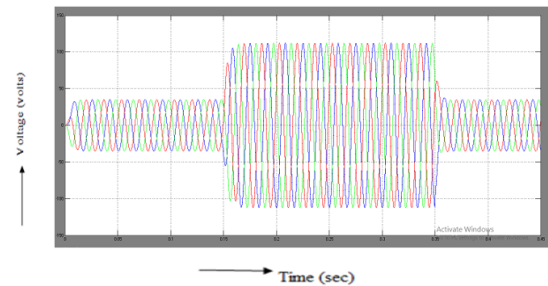


Fig.19 Absorbed voltages V_{ob2a} (blue), V_{ob2b} (red), and V_{ob2c} (green) during swell

5.3.4 Load voltage:

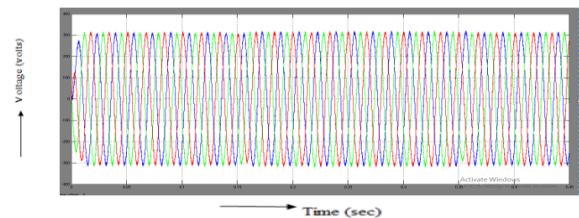


Fig.20 Load voltages V_{La} (blue), V_{Lb} (red), and V_{Lc} (green) during swell

5.3.5 Voltages of capacitor:

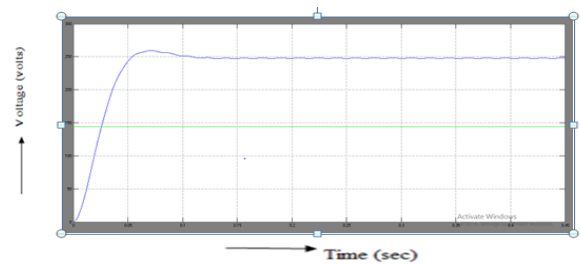


Fig.21 Voltages of dc-dc converter in Capacitor

44 μ F (Blue) and Capacitor 55F (Green) during voltage sag

5.3.6 Currents of capacitor:

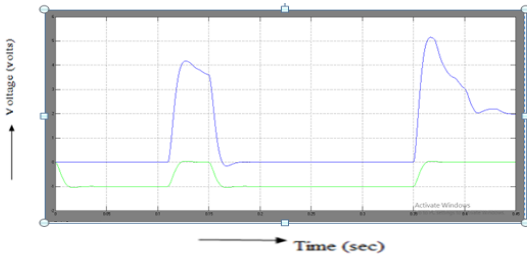


Fig.22 DC Link of DC-DC converter (Blue) and UCAP Current (Green) During Voltage Swell

5.3.7 Comparison of DVR voltage and system voltage:

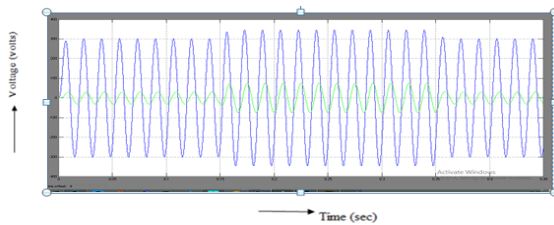


Fig.22 V_{ob2a} (green) and V_{sa} (blue) waveforms during swell

5.3.8 Active powers and RMS product of capacitor current and UCAP voltage:

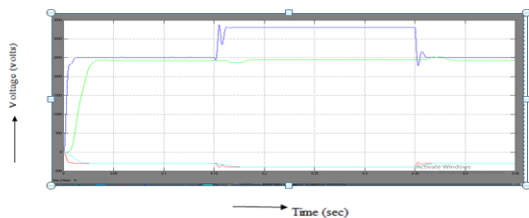


Fig.23 Active power of grid (Blue), Load (Green), inverter (Red) and RMS product of Capacitor current I_{dc} (DC-DC converter) and Ultra-capacitor voltage V_{dc} (Light blue) during voltage sag.

- From above table 5.1 it is clear that the existing method and proposed method gives same results under power quality constraints.

- In existing method PI controller depends K_p and K_i values by changing physically we get proper outputs.
- In proposed system to overcome this problem in modern days by replace PI controller with fuzzy logic controller we get outputs easily based on simple rules.
- In existing system PI controller operates only constant load and linear load and in proposed system fuzzy logic controller operates linear load, non-linear load, variable load, and constant load. When compare to PI controller the fuzzy logic controller is simple and logic and do not need any mathematical modeling.

Table 5.1 Comparison of Existing and proposed system

PARAMETERS	VOLTAGE SAG At (0.15 to 0.35)		VOLTAGE SWELL At (0.15 to 0.35)	
	Existing Method	Proposed Method	Existing Method	Proposed Method
Source and load peak voltages (P.U)	$V_{Smax}=0.535$ $V_{Lmax}=0.93$	$V_{Smax}=0.535$ $V_{Lmax}=0.93$	$V_{Smax}=1.23$ $V_{Lmax}=0.93$	$V_{Smax}=1.23$ $V_{Lmax}=0.93$
Source voltages	$V_{Sa}=181V$ $V_{Sb}=181V$ $V_{Sc}=181V$	$V_{Sa}=180V$ $V_{Sb}=180V$ $V_{Sc}=180V$	$V_{Sa}=415V$ $V_{Sb}=415V$ $V_{Sc}=415V$	$V_{Sa}=415V$ $V_{Sb}=415V$ $V_{Sc}=415V$
DVR voltages	$V_{inj2a}=157V$ $V_{inj2b}=157V$ $V_{inj2c}=157V$	$V_{inj2a}=158V$ $V_{inj2b}=158V$ $V_{inj2c}=158V$	$V_{ob2a}=77V$ $V_{ob2b}=77V$ $V_{ob2c}=77V$	$V_{ob2a}=77V$ $V_{ob2b}=77V$ $V_{ob2c}=77V$
Load voltages	$V_{La}=315V$ $V_{Lb}=315V$ $V_{Lc}=315V$	$V_{La}=317V$ $V_{Lb}=317V$ $V_{Lc}=317V$	$V_{La}=318V$ $V_{Lb}=318V$ $V_{Lc}=318V$	$V_{La}=319V$ $V_{Lb}=319V$ $V_{Lc}=319V$
Voltages of V_{dc} and UCAP	$V_{dc}=260V$ UCAP=144V	$V_{dc}=260V$ UCAP=144V	$V_{dc}=260V$ UCAP=144V	$V_{dc}=260V$ UCAP=144V

CONCLUSION

This project mainly concentrates to mitigate the voltage sags and swells by using a Fuzzy logic controller in DC-DC converter at the integration of UCAP-DVR. Voltage sag and voltage swell compensation of the distribution grid by this means improving the power quality. In the system the Ultra capacitor based rechargeable energy storage integrated to the DVR system to increase its voltage restoration capabilities. DVR is able to separately compensate voltage sag and swells without relying on the grid to compensate for faults. The control approach used is simple and is based on injecting voltages in-phase with the system voltage and is easier to implement when the DVR system has the ability to supply active power. Average current mode control is used to control the output voltage of the dc-dc converter due to its naturally stable

characteristics. In the existing method, PI controller is used as a controllers of both DC-DC converter and DVR. In the proposed system, fuzzy logic controller is used in DC-DC converter by replacing average current mode controller in order to reduce the mathematical modelling and can work with imprecise inputs and can handle linearities and non-linearities. Simulation of the ultra-capacitor, dc-dc converter and grid joined inverter is carried out using MATLAB and magnitudes of the waveforms is observed for voltage sag and swell conditions. In the proposed system fuzzy logic controller is used at the integration of UCAP-DVR is simulated and it reduced mathematical modelling when compared to existing system.

REFERENCES

- [1] N. H. Woodley, L. Morgan, and A. Sundaram, "Experience with an inverter-based dynamic voltage restorer," *IEEE Trans. Power Del.*, vol. 14, no. 3, pp. 1181–1186, Jul. 1999.
- [2] S. S. Choi, B. H. Li, and D.M. Vilathgamuwa, "Dynamic voltage restoration with minimum energy injection," *IEEE Trans. Power Syst.*, vol. 15, no. 1, pp. 51–57, Feb. 2000.
- [3] D. M. Vilathgamuwa, A. A. D. R. Perera, and S. S. Choi, "Voltage sag compensation with energy optimized dynamic voltage restorer," *IEEE Trans. Power Del.*, vol. 18, no. 3, pp. 928–936, Jul. 2003.
- [4] Y. W. Li, D. M. Vilathgamuwa, F. Blaabjerg, and P. C. Loh "A robust control scheme for medium-voltage-level DVR implementation," *IEEE Trans. Ind. Electron.*, vol. 54, no. 4, pp. 2249–2261, Aug. 2007.
- [5] A. Ghosh and G. Ledwich, "Compensation of distribution system voltage using DVR," *IEEE Trans. Power Del.*, vol. 17, no. 4, pp. 1030–1036, Oct. 2002.
- [6] A. Elnady and M. M. A. Salama, "Mitigation of voltage disturbances using adaptive perception-based control algorithm," *IEEE Trans. PowerDel.*, vol. 20, no. 1, pp. 309–318, Jan. 2005.
- [7] P. R. Sanchez, E. Acha, J. E. O. Calderon, V. Feliu, and A. G. Cerrada, "A versatile control scheme for a dynamic voltage restorer for power quality improvement," *IEEE Trans. Power Del.*, vol. 24, no. 1, pp. 277–284, Jan. 2009.
- [8] C. S. Lam, M. C. Wong, and Y. D. Han, "Voltage swell and overvoltage compensation with unidirectional power flow controlled dynamic voltage restorer," *IEEE Trans. Power Del.*, vol. 23, no. 4, pp. 2513–2521, Oct. 2008.
- [9] K. Sahay and B. Dwivedi, "Supercapacitor energy storage system for power quality improvement: An overview," *J. Elect. Syst.*, vol. 10, no. 10, pp. 1–8, 2009.
- [10] P. F. Ribeiro, B. K. Johnson, M. L. Crow, A. Arsoy, and Y. Liu, "Energy storage systems for advanced power applications," *Proc. IEEE*, vol. 89, no. 12, pp. 1744–1756, Dec. 2001.
- [11] H. K. Al-Hadidi, A. M. Gole, and D. A. Jacobson, "A novel configuration for a cascaded inverter-based dynamic voltage restorer with reduced energy storage requirements," *IEEE Trans. Power Del.*, vol. 23, no. 2, pp. 881–888, Apr. 2008.
- [12] R. S. Weissbach, G. G. Karady, and R. G. Farmer, "Dynamic voltage compensation on distribution feeders using flywheel energy storage," *IEEE Trans. Power Del.*, vol. 14, no. 2, pp. 465–471, Apr. 1999.
- [13] A. B. Arsoy, Y. Liu, P. F. Ribeiro, and F. Wang, "StatCom-SMES," *IEEE Ind. Appl. Mag.*, vol. 9, no. 2, pp. 21–28, Mar. 2003.
- [14] C. Abbey and G. Joos, "Supercapacitor energy storage for wind applications," *IEEE Trans. Ind. Appl.*, vol. 43, no. 3, pp. 769–776, Jun. 2007.
- [15] S. Santoso, M. F. McGranaghan, R. C. Dugan, and H.W. Beaty, *Electrical Power Systems Quality*, 3rd ed. New York, NY, USA: McGraw-Hill, Jan. 2012.
- [16] Y. Chen, J. V. Mierlo, P. V. Bosschet, and P. Lataire, "Using super capacitor based energy storage to improve power quality in distributed power generation," in *Proc. IEEE Int. Power Electron. Motion Control Conf.(EPE-PEMC)*, 2006, pp. 537–543.
- [17] Y. Li, Y. Wang, B. Zhang, and C. Mao, "Modeling and simulation of dynamic voltage restorer based on supercar acitor energy storage," in *Proc. Int. Conf. Electric Mach. Syst. (ICEMS)*, 2008, pp. 2064–2066.
- [18] H. Akagi, E. H.Watanabe, and M. Aredes, *Instantaneous Reactive Power Theory and Applications to Power Conditioning*, 1st ed. Hoboken, NJ,USA: Wiley, Piscataway, NJ, USA: IEEE Press, 2007.
- [19] R. W. Erickson and D. Maksimovic, *Fundamentals of Power Electronics*, 2nd ed. Norwell, MA, USA: Kluwer, 2001.



Mr.V.Yuvaraj has pursuing her Master of Technology in Power Systems, EEE Department, SREE VIDHYANIKETHAN, Tirupati, Andhra Pradesh, India.



D.SREENIVASULU REDDY received B.Tech degree in Electrical and Electronics Engineering from JNT University Hyderabad and M.Tech degree in Electrical Power System from from JNT University, Anapatpur. Presently working as Assistant Professor in SreeVidyanikethan Engineering College, Tirupathi. His research areas are power system stability and control.